Methanol Steam Reforming

DOI: 10.1002/anie.201209587

High CO_2 Selectivity in Methanol Steam Reforming through ZnPd/ZnO Teamwork**

*Matthias Friedrich, Simon Penner, Marc Heggen, and Marc Armbrüster**

Methanol steam reforming (MSR; $CH_3OH + H_2O \rightarrow 3H_2 + CO_2$) is considered an important building block in the future energy infrastructure to provide clean hydrogen for fuel cell applications.[1] The suppression of CO is the greatest challenge, as the subsequently used fuel cell catalysts only tolerate CO concentrations of up to 50 ppm.[2] Pd/ZnO catalysts have been shown to compete with Cu-based catalysts,[3,4] and have set benchmarks at about 1000 ppm CO. The formation of the intermetallic compound ZnPd on the ZnO support is held responsible for the high CO_2 selectivity.[5–11] However, no proof of the origin of high CO_2 selectivity has been reported thus far. Unraveling the structural properties that account for the selectivity of this catalyst would definitely aid in improving MSR catalysts for practical application. Recently, detailed characterization of the single constituents (unsupported ZnPd[12] and pure ZnO[13]) in MSR resulted in the justified proposal of a bifunctional synergism between intermetallic and oxidic species, which leads to a highly active interface that is necessary for the outstanding selectivity of ZnPd/ZnO catalysts. The bulk composition of ZnPd affects its surface composition and also determines the oxidizability of Zn on the surface.[12] The presence of oxidized Zn in near-surface regions has been shown to be inevitably linked to a high CO_2-selectivity in inverse model catalyst studies of near-surface intermetallic phases.[14–16] The knowledge transfer from these model systems to high-performance catalysts represents a great step towards understanding MSR.

Herein we reveal the origin of the high CO_2 selectivity of ZnO-supported ZnPd particles in MSR by linking the catalytic properties of ZnPd/ZnO, especially in the initial phase on-stream, with aberration-corrected high-resolution transmission electron microscopy (HRTEM) imaging of the catalyst at different stages of the MSR reaction.

[*] M. Friedrich, Dr. M. Armbrüster
Max-Planck-Institut für Chemische Physik fester Stoffe
Nöthnitzer Straße 40, 01097 Dresden (Germany)
E-mail: research@armbruester.net
Dr. S. Penner
Institute of Physical Chemistry, University of Innsbruck
Innrain 52A, 6020 Innsbruck (Austria)
Dr. M. Heggen
Ernst Ruska-Centrum und Peter Grünberg Institut
Forschungszentrum Jülich, 52425 Jülich (Germany)

[**] This work was financially supported by the DFG (AR 617/3-1) and the Austrian Science Foundation (P20892-N19, F4503-N16). Networking within the COST Action CM0904 nurtured this publication.

Supporting information for this article is available on the WWW under http://dx.doi.org/10.1002/anie.201209587.

ZnPd/ZnO was first examined by TEM and scanning TEM (STEM) after reductive treatment at 773 K (state I). The sample consists of intermetallic particles (ca. 5–50 nm in size) that can be clearly discriminated from the ZnO support (Supporting Information, Figure S3). Figure 1 shows a representative HRTEM image of a single ZnPd particle attached to a larger ZnO grain. Lattice fringes of 2.2 Å, corresponding to the ZnPd (101) lattice distance (theoretical spacing: 2.18 Å),[17] are observed. Smaller lattice fringes (1.3 Å), are also visible and correspond to the ZnPd (112) lattice distance (theoretical spacing: 1.29 Å).[17] Most significantly, the particle exhibits straight edges and no surface layer or particles covering the ZnPd particle could be detected. A highly defective internal structure and overall polycrystalline nature are typical for the ZnPd particles in state I. Stacking faults, grain boundaries, and bending of individual lattice planes are frequently observed. Although broad low-intensity reflections of elemental palladium were found by XRD (Figure S2), no palladium particles were detected in the analyzed TEM images, which makes them most likely to be encapsulated in the ZnO support; thus, they will not contribute to catalysis.

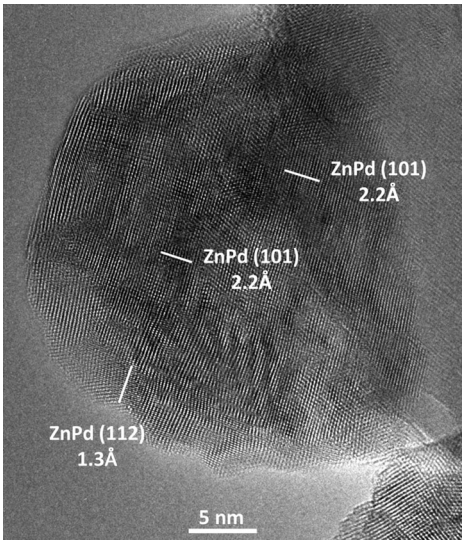

Figure 1. HRTEM image of a single polycrystalline ZnPd particle in state I. The (101) and (112) lattice fringes of the tetragonal ZnPd structure are indicated.

As the corresponding STEM experiments reveal, these structural defects are not the only ones observed. In general, after reduction all of the ZnPd particles are also chemically inhomogeneous, as is shown by an overview high-angle annular dark-field (HAADF) STEM image of the ZnPd

particles in state I (Figure S4). Figure 2a highlights a STEM image of a single ZnPd particle and reveals strong internal HAADF contrast variation. The particle is attached to a single ZnO grain and exhibits homogeneous HAADF contrast. As the HAADF intensity is roughly proportional to $Z^{1.5-2}$ (depending on the camera length of the microscope and constant thickness and density provided), heavier elements appear brighter and lighter ones darker. Thus, the ZnPd particles reveal a variation in chemical composition involving palladium-enriched and -depleted zones. This is corroborated by the corresponding EEL line scan experiments. Figure 2b compares the EEL intensities for Zn, Pd, and O atoms with the measured HAADF intensity. In general, it can be noted that the Pd and Zn signals both increase at the edge of the particle; however, both show different behavior within the particle. For example, at a distance of 10 nm from the starting point, the Pd signal shows a minimum and the Zn signal shows a local maximum. This result accounts for the chemical inhomogeneity of the particles in state I. Owing to Z-contrast-like behavior of the HAADF signal, the heavy Pd atoms contribute more to the HAADF signal than Zn. This is why the HAADF signal in Figure 2b shows a local minimum at 10 nm, which indicates a local Pd depletion zone.

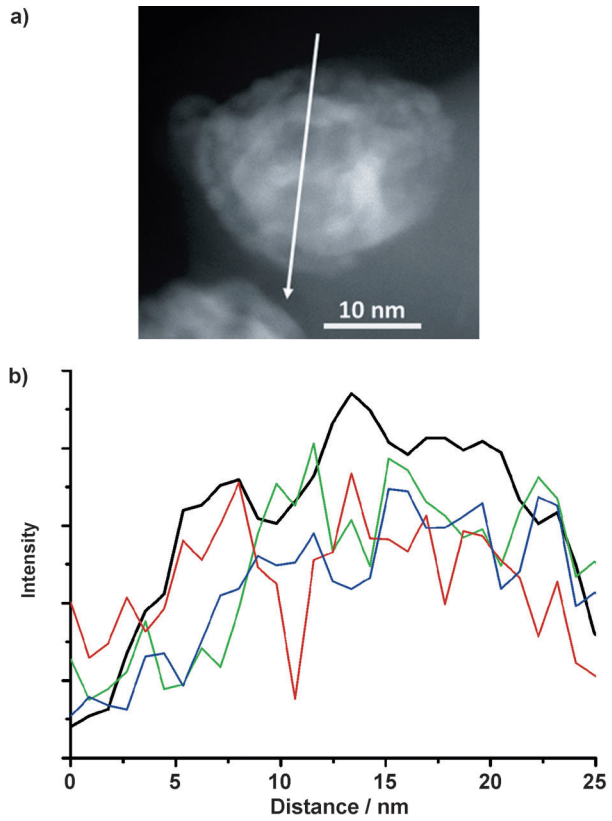

Figure 2. a) HAADF-STEM image of a single ZnPd particle after reduction (state I). The arrow indicates the line along which the EEL spectra were recorded. b) Characteristics of the HAADF intensity (——) compared with the corresponding intensity profiles of Pd (Pd-M EELS; ——), Zn (Zn-$L_{2,3}$ EELS; ——), and O (O-K EELS; ——) atoms, as extracted from the corresponding EEL edges.

The ZnPd/ZnO catalyst was reduced after loading it in the reactor and was subsequently tested in MSR. The first experiment consisted of an isothermal MSR test performed at 523 K. Figure 3 shows the time-dependent development of methanol conversion and CO_2 selectivity in the first 20 h on stream. Although there is only a minor decrease in conversion over 20 h, low CO_2 selectivity (< 40 %) is clearly visible in the beginning of the reaction and increases steeply during the first 2 h until a stable selectivity of 97 % is reached, a value which is in agreement with the reported selectivity for this catalyst.[5–10] To our knowledge, this is the first time that a major change in CO_2 selectivity with increasing time-on-stream is reported for ZnPd/ZnO. The catalyst must have changed under MSR conditions until it reached an equilibrium state that is highly selective to CO_2. After 20 h on stream, the MSR atmosphere was switched off and the initial reduction conditions were applied again. Subsequently, MSR was conducted as before at 523 K, and showed the same initial behavior. In accordance with the electron microscopy studies, the fully reduced catalyst (state I) is apparently rather unselective for CO_2, and is only rendered selective in the reactive MSR atmosphere. Switching the catalyst from a selective to an unselective state can be achieved by applying the reductive conditions again.

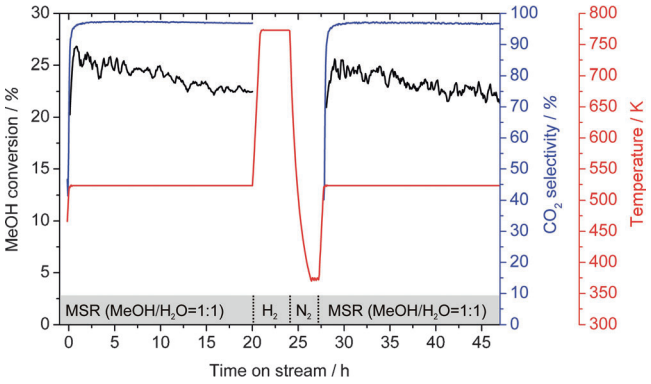

Figure 3. Methanol conversion and CO_2 selectivity of freshly reduced ZnPd/ZnO in MSR under isothermal conditions at 523 K. Reduction and purging after 20 h on stream was performed under the same conditions as before the reaction (see the Experimental Section). The gas atmospheres applied are shown at the bottom of the graph.

To exclude the possibility that the observed effects are caused by the chosen reaction temperature (523 K), a heating/cooling cycle under MSR conditions was conducted on a new sample from the same batch after pretreatment by identical calcination and reduction processes. The MSR test ranged from 423 K to 673 K and back to 423 K, with the temperature changed at a rate of 2 K min^{-1} (Figure 4). As expected, methanol conversion increased with increasing temperature. As both the heating and cooling curves follow exactly the same trend, pronounced deactivation due to sintering or carbon deposition can be excluded.

Because of the low conversion at low reaction temperatures, selectivity determination is only reasonable above 475 K. At the beginning of the MSR experiment, the CO_2

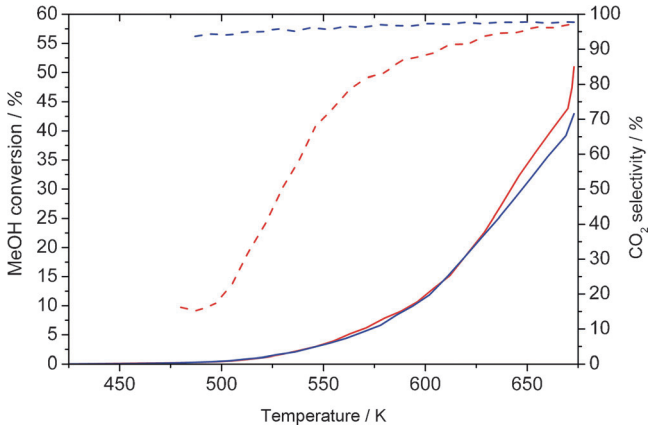

Figure 4. Methanol conversion and CO_2 selectivity of the freshly reduced ZnPd/ZnO catalyst in MSR during heating and cooling at a rate of 2 K min^{-1} from 423 to 673 K. MeOH conversion during heating (——), MeOH conversion during cooling (——), CO_2 selectivity during heating (– – –), CO_2 selectivity during cooling (– – –).

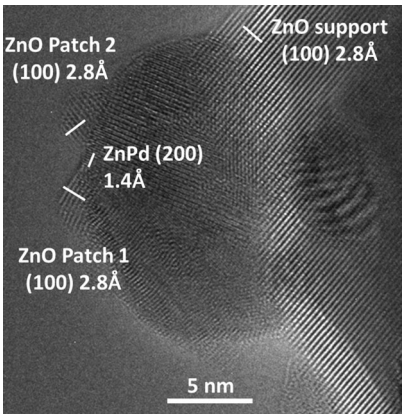

Figure 5. HRTEM image of a single ZnPd particle (state II) with two ZnO patches on the surface, both exhibiting ZnO(100) lattice fringes of 2.8 Å. The ZnO support is also clearly visible with lattice spacings of 2.8 Å. The ZnPd lattice distances (measured at 1.4 Å) can be assigned to the (200) lattice planes.

selectivity of the freshly reduced catalyst was very poor (ca. 15%). With increasing temperature, the CO_2 selectivity steadily increased to >97%. The selectivity consistantly remained above 95% during cooling. Again, a major increase in selectivity is observed owing to significant change in the ZnPd/ZnO catalyst with time on stream during the initial heating, but not during cooling, thus revealing the irreversible nature of the change under MSR conditions.

In light of the temperature-dependent MSR measurements it is even more evident that the unselective state of the catalyst in the beginning of the experiment is due to the presence of fully reduced intermetallic ZnPd particles on the ZnO support, whereas the highly selective state after 2 h on stream may be due to at least partially oxidized ZnPd particles establishing a synergistic ZnPd–ZnO interface.

To clearly identify the structural properties of ZnPd/ZnO in the highly selective state, after the temperature-dependent MSR test the catalyst was investigated by electron microscopy (state II). As with the sample of the state I catalyst, overview imaging of the sample of the state II catalyst (Figure S3) shows intermetallic ZnPd particles (5–50 nm) on the ZnO support, thus excluding significant sintering. In contrast, HRTEM and HAADF analyses revealed significant differences. Figure 5 shows a typical individual ZnPd particle on ZnO, the appearance of which is now strikingly different than that of the particles in state I. Although the individual lattice fringes of the ZnPd structure can be easily discriminated (for example, those of the (200) lattice with distances of 1.4 Å), as can those of the ZnO support (for example, those of the (100) lattice with distances of 2.8 Å), patches with different contrast and well-defined lattice fringes appear on the surface of the ZnPd particles. These patches can be exclusively assigned to those of the ZnO structure based on the (100) lattice planes with distances of 2.8 Å. Elemental palladium, as identified by broad low-intensity reflections in XRD (Figure S2), were again undetectable by TEM.

The presence of oxidized Zn patches on the intermetallic ZnPd particles is corroborated by HAADF imaging of

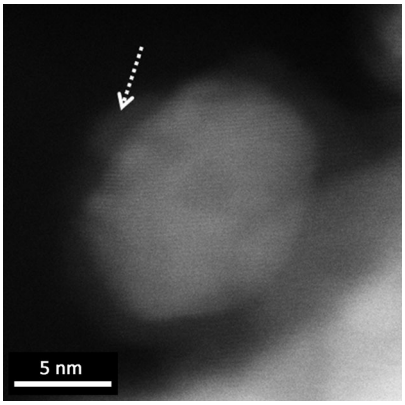

Figure 6. HAADF-STEM image of a single ZnO-covered ZnPd particle (state II). The arrow indicates a region on the particle surface with lower Z-contrast than the ZnPd particle, which is consistent with the absence of Pd and the presence of a ZnO patch.

individual particles. Figure 6 shows a representative ZnO-covered ZnPd particle with atomic resolution. In accordance with the weaker Z-contrast of zinc versus palladium, the ZnO patches display a darker contrast next to the brighter ZnPd particle. The ZnPd particles are chemically more homogeneous in state II, because the strong alternating HAADF contrast that was observed before reaction (state I) is absent.

These observations indicate that the appearance of the oxidized Zn species is linked to the observation of high CO_2 selectivity (see Figure 3 and 4). Ultimately, these results confirm previous studies on related model systems wherein oxidized Zn species have been clearly identified by in situ X-ray photoelectron spectroscopy as being present in the CO_2-selective state of the catalyst, and as being capable of efficient water activation, a prerequisite for a CO_2-selective catalyst.[12,14–16] Nevertheless, XPS is often not suitable for exploring supported catalysts such as ZnPd/ZnO, because of the induced charging on insulating samples and the excess of ZnO that makes it impossible to identify ZnO patches formed in situ.

This is the first time that the selective state of a ZnPd/ZnO catalyst is made clearly visible and is shown to contain special interfacial sites, where uncovered intermetallic ZnPd particles and ZnO coexist in close proximity. Most presumably, these patches are formed by partial oxidation of the corresponding ZnPd particles under MSR conditions, as shown by earlier studies of unsupported ZnPd,[12] rather than being transported away from the ZnO bulk support. The partial coverage of the ZnPd particles by ZnO can be explained by a quasi-equilibrium under these MSR conditions, as the methanol/water feed coexists with the produced H_2, thus forming a reductive/oxidative atmosphere and hindering the complete oxidation of the ZnPd particles. The teamwork between ZnO and ZnPd is not only detectable by this TEM study, but is further corroborated by comparing the apparent activation energies of ZnO (144 kJ mol^{-1} [13]), unsupported ZnPd (120 kJ mol^{-1} [12]), and the present ZnPd/ZnO catalyst. With an apparent activation energy of only 75 kJ mol^{-1} for this catalyst, the synergistic effect of the teamwork is easily discernible.

In summary, by means of a combination of catalytic studies and high-resolution transmission electron microscopy, we have shown that the highly CO_2-selective state of ZnPd/ZnO catalysts for methanol steam reforming is not due to the mere formation of ZnPd on ZnO. In fact, the in situ partial oxidation of the ZnPd nanoparticles leads to a large interface between intermetallic ZnPd and small ZnO patches, thus improving the ability of the material to activate water, which results in the high CO_2 selectivity. The question of whether a spillover at the formed interface is responsible for the high performance of the catalyst, or if the key reaction steps take place with an increased rate at the interface itself, still remains open.

Experimental Section

For catalytic and electron microscopy studies, a Pd/ZnO (9.2 wt.%) powder catalyst was prepared following a standard incipient-wetness technique, in close analogy to Ref. [5]. Reductive pretreatment to induce the formation of ZnPd was performed at 773 K in H_2 (5 vol.%). The catalytic experiments were performed in a CH_3OH/H_2O (1:1) mixture up to 673 K. Pre- and post-reaction analysis of the catalyst was done by XRD. Aberration-corrected electron microscopy was performed on samples after the respective treatments in the reactor, with only short contact to air for transfer to the electron microscope. For further experimental details, see the Supporting Information.

Received: November 30, 2012
Revised: February 6, 2013
Published online: March 11, 2013

Keywords: Methanol · nanoparticles · palladium · synergistic effects · zinc

[1] *Die Zukunft der Energie* (Eds.: P. Gruss, F. Schüth), C. H. Beck, München, **2008**.
[2] H.-F. Oetjen, V. M. Schmidt, U. Stimming, F. Trila, *J. Electrochem. Soc.* **1996**, *143*, 3838 – 3842.
[3] J.-P. Shen, C. Song, *Catal. Today* **2002**, *77*, 89 – 98.
[4] H. Purnama, T. Ressler, R. E. Jentoft, H. Soerijanto, R. Schlögl, R. Schomäcker, *Appl. Catal. A* **2004**, *259*, 83 – 94.
[5] N. Iwasa, S. Masuda, N. Takezawa, *React. Kinet. Catal. Lett.* **1995**, *55*, 349 – 353.
[6] A. M. Karim, T. Conant, A. K. Datye, *Phys. Chem. Chem. Phys.* **2008**, *10*, 5584 – 5590.
[7] T. Conant, A. M. Karim, V. Lebarbier, Y. Wang, F. Girgsdies, R. Schlögl, A. Datye, *J. Catal.* **2008**, *257*, 64 – 70.
[8] A. Karim, T. Conant, A. Datye, *J. Catal.* **2006**, *243*, 420 – 427.
[9] E. A. Ranganathan, S. K. Bej, L. T. Thompson, *Appl. Catal. A* **2005**, *289*, 153 – 162.
[10] Y. H. Chin, R. Dagle, J. Hu, A. C. Dohnalkova, Y. Wang, *Catal. Today* **2002**, *77*, 79 – 88.
[11] K. Föttinger, J. A. van Bokhoven, M. Nachtegaal, G. Rupprechter, *J. Phys. Chem. Lett.* **2011**, *2*, 428 – 433.
[12] M. Friedrich, D. Teschner, A. Knop-Gericke, M. Armbrüster, *J. Catal.* **2012**, *285*, 41 – 47.
[13] H. Lorenz, M. Friedrich, M. Armbrüster, B. Klötzer, S. Penner, *J. Catal.* **2013**, *297*, 151 – 154.
[14] C. Rameshan, C. Weilach, W. Stadlmayr, S. Penner, H. Lorenz, M. Hävecker, R. Blume, T. Rocha, D. Teschner, A. Knop-Gericke, R. Schlögl, D. Zemlyanov, N. Memmel, G. Rupprechter, B. Klötzer, *J. Catal.* **2010**, *276*, 101 – 113.
[15] C. Rameshan, W. Stadlmayr, C. Weilach, S. Penner, H. Lorenz, M. Hävecker, R. Blume, T. Rocha, D. Teschner, A. Knop-Gericke, R. Schlögl, N. Memmel, D. Zemlyanov, G. Rupprechter, B. Klötzer, *Angew. Chem.* **2010**, *122*, 3292 – 3296; *Angew. Chem. Int. Ed.* **2010**, *49*, 3224 – 3227.
[16] C. Rameshan, W. Stadlmayr, S. Penner, H. Lorenz, N. Memmel, M. Hävecker, R. Blume, D. Teschner, T. Rocha, D. Zemlyanov, A. Knop-Gericke, R. Schlögl, B. Klötzer, *Angew. Chem.* **2012**, *124*, 3057 – 3061; *Angew. Chem. Int. Ed.* **2012**, *51*, 3002 – 3006.
[17] M. Friedrich, A. Ormeci, Yu. Grin, M. Armbrüster, *Z. Anorg. Allg. Chem.* **2010**, *636*, 1735 – 1739.

